Geochimica et Cosmochimica Acta 360 (2023) 231–240

Contents lists available at ScienceDirect

Geochimica et Cosmochimica Acta

journal homepage: www.elsevier.com/locate/gca

The chondritic impactor origin of the Ni-rich component in Australasian tektites and microtektites

L. Folco [a,b,*], P. Rochette [c], M. D'Orazio [a,b], M. Masotta [a,b]

[a] Dipartimento di Scienze della Terra, Università di Pisa, Via S. Maria 53, Pisa, Italy
[b] CISUP, Centro per la Integrazione della Strumentazione dell'Università di Pisa, Lungarno Pacinotti, Pisa, Italy
[c] Aix-Marseille Université, CNRS, IRD, INRAE, UM 34 CEREGE, Aix-en-Provence, France

ARTICLE INFO

Associate editor: Tomas Magna

Keywords:
Tektites
Microtektites
Impact melting
Impact cratering
Geochemistry
Australasian tektite strewn field

ABSTRACT

In the Earth's crust, Ni is generally concentrated in mafic and ultramafic rocks and is coupled with Mg in Mg-olivine, Mg-pyroxene and spinel. Whether the Ni-rich, and in general, the mafic component of Australasian tektites and microtektites is terrestrial or meteoritic is still debated. To test the origin of the Ni-rich component, we studied the Ni versus Mg distribution in a large geochemical database of Australasian tektites (n = 208) and microtektites (n = 238) from the literature. Nickel contents of up to 428 μg/g in tektites and 678 μg/g in microtektites covary with Mg in tektites and in most (~85%) of the microtektites defining a mixing trend between crustal and chondritic values, thereby documenting the chondritic origin of the Ni-rich component in Australasian tektites/microtektites. Mixing calculations indicate up to 4% and up to 6% by weight chondritic component in tektites and microtektites, respectively. A possible mafic component of terrestrial origin is observed in a minority of tektite and microtektite specimens. This finding is consistent with previous works suggesting a possible occurrence of a chondritic signature in high-Ni tektites, based on the study of highly siderophile elements and Os isotopes, and high-Ni microtektites, based on Ni, Co, and Cr ratios. The combined geochemical and isotopic analyses of high-Ni tektites and microtektites in collections worldwide may thus reveal the chondritic impactor type that generated one of the presumably largest impacts in the Cenozoic.

1. Introduction

Impact melt rocks produced by hypervelocity impacts of asteroidal or cometary bodies onto Earth's crust can incorporate small amounts of meteoritic material, resulting in distinct chemical signatures relative to local or average continental crust values (Koeberl et al., 2012; Goderis et al., 2013). Identifying the impactor signature is a geochemical challenge due to its considerable dilution by the much larger amount of target-derived melt. Dilution is typically in the order of ~1:100 by weight (e.g., Koeberl et al., 2012; Goderis et al., 2013) reaching ~10:100 in some cases (e.g., Fazio et al., 2016). Disequilibrium melting, multicomponent mixing/mingling, melt fragmentation, solid–liquid-gas chemical and isotopic fractionation during impact melting and cooling are additional complicating factors. Identifying such signature can provide important clues on the impactor type, thereby enabling investigation of the flux of different kinds of impactors to Earth, their orbital evolution from their source regions and the collisional/disintegration history of their asteroidal/cometary parent bodies (Tagle and Claeys, 2005; Goderis et al., 2013; Schmitz, 2013). Tracing the impactor signature in impact melt rocks can also provide significant insights into the poorly known physical–chemical interaction between target and projectile upon impact melting at their initial contact (Ebert et al., 2014; Fazio et al., 2016; Goderis et al., 2017; Hamann et al., 2018).

The nature of the impactor that generated the Australasian tektite/microtektite (high velocity ejecta of glassy impact melt masses of siliceous composition) strewn field is an outstanding issue. Its identification would significantly add to the set of parameters required to constrain the scenario of one of the largest and enigmatic impacts in the Cenozoic. The impact produced the largest of the five known Cenozoic tektite/microtektite strewn fields (i.e., North American, Central European, Ivory Coast, Australasian and Central American; e.g., Glass and Simonson, 2013; Rochette et al., 2021), covering more than 15% of the Earth's surface. Despite being the youngest strewn field (~0.79 million years-old; Schwarz et al., 2016; Jourdan et al., 2019; Di Vincenzo et al., 2021), it is the only one without an associated crater to date (Glass and Simonson, 2013), although estimates point to a large crater at least 30

* Corresponding author.
E-mail address: luigi.folco@unipi.it (L. Folco).

https://doi.org/10.1016/j.gca.2023.09.018
Received 28 March 2023; Accepted 21 September 2023
Available online 23 September 2023

km in diameter (Glass and Koeberl, 2006), possibly located in Indochina (e.g., Ma et al., 2004) or in Northwest China (Mizera et al., 2022). The identification of an impactor signature would also contribute to the long-standing discussion on the tektite – microtektite formation processes, to which research on the Australasian strewn field continues to provide new fundamental clues and input for modelers (e.g., Glass and Pizzuto, 1994; Ma et al., 2004; Prasad et al., 2007; Folco et al., 2010a,b; Goderis et al., 2017; Cavosie et al., 2017; Rochette et al., 2018; Gattacceca et al., 2021; Masotta et al., 2020).

In our previous work (Folco et al., 2018), we identified a chondritic impactor signature in 33 Australasian microtektites (size range: 200–700 μm) from within 3000 km of one of the hypothetical impact location in Indochina (~17° N, 107° E; Ma et al., 2004; Fig. 1). They have Ni, Co and Cr concentrations above continental crust values, i.e., up to 680, 50 and 370 μg/g, respectively (Ni, Co, Cr values for the upper continental crust, UCC, and bulk crust are 20–105, 10–29 and 35–185 μg/g, respectively; Taylor and McLennan, 1995). We also showed that Cr, Co and Ni are positively correlated and that the Cr/Ni versus Co/Ni ratios are consistent with mixing between continental crust and an ordinary chondrite (LL chondrite) composition. An impactor signature of broadly chondritic composition was proposed earlier by Goderis et al. (2017) on the basis of Cr and Ir elemental ratios and unfractionated CI-normalized highly siderophile element (HSE) patterns in Australasian tektites enriched in Ni (100–428 μg/g). Ackerman et al. (2019) later suggested addition (<1 wt%) of a chondritic impactor in four Australasian tektites enriched in Ni (99–166 μg/g Ni) based on Re-Os isotope systematics. However, these results were recently questioned by Sieh et al. (2020), who linked the Ni, Co, Cr and HSE concentrations in Australasian tektites to a mafic terrestrial component, following previous work on platinum group elements in tektites – published in abstract form – by Shirai et al. (2016) and on Ni-Co-Cr interrelations in 26 layered (Muon-Nong type) tektites with Ni < 130 μg/g from Indochina (Wasson, 1991). In particular, Sieh et al. (2020) suggested that this mafic terrestrial component was provided by the basalts of the Bolaven Plateau in southern Laos. However, major element and Sr-Nd isotope mixing models, using the Bolaven basalts and the underlying Mesozoic sandstones as endmembers, do not reproduce the average composition of the Australasian tektites (Mizera, 2022).

Nickel is significantly present in mafic, mantle and mantle-derived rocks, i.e., peridotites and basalts. In these rocks, it is coupled with Mg in Mg-olivine, Mg-pyroxene, and spinel, in concentrations up to 3000 μg/g (e.g., Gall et al., 2017). Using a large geochemical data base of Australasian tektites (n = 208) and microtektites (n = 238) from the literature, we have studied the relationship between Ni and Mg concentrations to provide new insights into the impactor signature.

2. The geochemical data set

The data set used in this work includes the major and trace element compositions of all the tektites and microtektites so far published in the literature (to the best of our knowledge) for which Mg, Cr, Co and Ni contents are available (Tables 1, 2, SM1, and SM2).

The tektite data set includes 225 analyses from 210 individual tektites (Chapman and Scheiber, 1969; Son and Koeberl, 2005; Amare and Koeberl, 2006; Mizera et al., 2016; Goderis et al., 2017; Žák et al., 2019), with Ni contents up to 428 μg/g (Goderis et al., 2017). Tektites belong to the three structural types: Muong Nong-, splash-form- and ablated-types and were recovered from Vietnam, Laos, Cambodia, Thailand, South China, Indonesia, Philippines and Australia. Elemental concentrations were obtained using atomic absorption spectroscopy (AAS) in the late

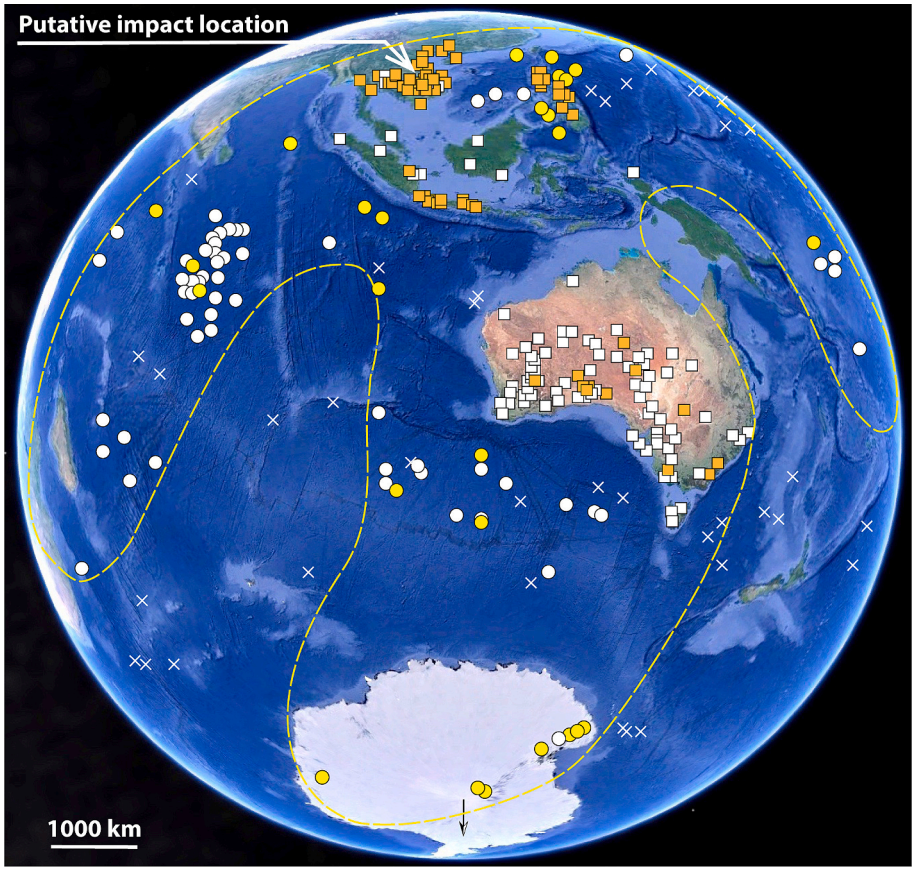

Fig. 1. The Australasian tektite/microtektite strewn field (modified after Di Vincenzo et al., 2021). The find locations of tektites and microtektites are marked by squares and circles, respectively. The orange and yellow symbols indicate the find locations of the tektite and microtektite specimens studied in this work (see also Tables 1 and 2). White crosses are sites in the ocean where microtektites were not found. The putative impact location in Indochina (Ma et al., 2004) is arrowed.

Table 1
Find locations and shape types of the Australasian tektites studied in this work.

Locality	*Muong Nong*	*Splash-form*	*Ablated splash-form*	*Unspecified*	*Totals*	*Method*	*References*
Australia		4	2	5	11	INAA, IPAA	[1, 2]
Cambodia	3	4			7	INAA, IPAA, LA-ICP-MS	[1, 2, 3]
China	1	3			4	INAA, IPAA	[1, 2]
Indonesia		8		9	17	LA-ICP-MS, IPAA, INAA	[1, 2, 3]
Laos	15	3			18	EPMA, INAA, IPAA	[1, 2, 4]
Philippines		6		19	25	EPMA, INAA	[1, 2, 5]
Thailand	5	4		1	10	INAA, IPAA	[1, 2]
Vietnam	8	108		2	118	EPMA, INAA	[2, 3, 5, 6]
Totals	32	140	2	36	210		

References: [1] Chapman and Scheiber (1969); [2] Mizera et al. (2016); [3] Goderis et al. (2017); [4] Žák et al. (2019); [5] Son and Koeberl (2005); [6] Amare and Koeberl (2006).

Table 2
Find locations and compositional types of the Australasian microtektites studied in this work.

Site/Core	*Locality*	*Lat*	*Long*	*Normal*	*Int-Mg*	*High-Mg*	*High-Al*	*High-Ni*	*High-Fe*	*Totals*	*Reference*
Allan Hills	Antarctica	−76.74	159.39	6						6	[1]
DSDP 213	Indian Ocean, SW of Sumatra	−10.21	93.90	2		1				3	[2]
DSDP 292	Philippine Sea	15.82	124.65	2						2	[2]
DSDP 293	Philippine Sea	20.34	124.09	1						1	[2]
DSDP 294	Philippine Sea	22.58	131.38	1						1	[2]
E45-71	Indian Ocean	−48.02	114.49	1	2		1			4	[2]
E45-89	Indian Ocean	−39.52	114.47	3		1				4	[2]
E49-50	Indian Ocean	−40.61	99.91	2						2	[2]
Frontier Mountain	Antarctica	−72.98	160.33	2		1				3	[3, 4]
Killer Nunatak	Antarctica	−71.90	160.47	1						1	[1]
Larkman Nunatak	Antarctica	−85.77	179.38	4	3	2	1			10	[5]
Miller Butte	Antarctica	−72.70	160.25	17	4	6	1			28	[1]
Mount Raymond	Antarctica	−85.88	174.72	30	8	2	2			42	[6]
Mt. Widerø	Antarctica	−72.15	23.26	33						33	[7]
ODP 1144	South China Sea	20.05	117.42	17					1	18	[8]
ODP 292	Philippine Sea	15.82	124.65	1						1	[2]
ODP 758B	Indian Ocean, NW of Sumatra	5.38	90.36	7				5		12	[2, 9]
ODP 767B	Celebes Sea	4.79	123.50	1				4		5	[9]
ODP 768B	Sulu Sea	8.00	121.22	6	1			6		13	[2, 9]
ODP 769A	Sulu Sea	8.79	121.22	2	1			5		8	[2, 9]
RC12-331	Indian Ocean	2.50	69.87			1				1	[2]
RC14-23	Indian Ocean	−9.18	76.76	1						1	[2]
RC14-46	Indian Ocean, SW of Sumatra	−7.82	100.00	1		1		6		8	[2]
Schroeder Spur	Antarctica	−71.63	160.50	8						8	[1]
SO95-17957–2	South China Sea	10.90	115.31	2				3		5	[9]
V16-76	Indian Ocean	−25.15	59.90	1	1					2	[2]
V19-153	Indian Ocean, SW of Sumatra	−8.85	102.12	5				2		7	[2]
V28-238	Pacific Ocean	1.02	160.48	1						1	[2]
V29-43	Indian Ocean	−12.33	75.08	1	1					2	[2]
Totals				158	22	15	6	31	1	233	

References: [1] Folco et al. (2016); [2] Glass et al. (2004); [3] Folco et al. (2008); [4] Folco et al. (2009); [5] van Ginneken et al. (2018); [6] Brase et al. (2021); [7] Soens et al. (2021); [8] Glass and Koeberl (2006); [9] Folco et al. (2018).

1960's (Chapman and Scheiber, 1969) and later by the combination of electron probe microanalyzer (EPMA), instrumental neutron or photon activation analyses (INAA or IPAA) (Son and Koeberl, 2005; Amare and Koeberl, 2006; Mizera et al., 2016; Goderis et al., 2017; Žák et al., 2019). Tektites analyzed by Chapman and Scheiber (1969) were classified into chemical groups, including high-Mg, high-Ca, low-Ca-high-Al and high-Cu,B. This classification is no longer in use, however, in this work, we will consider the high-Mg tektites (n = 10) separately, since some of them have compositions that deviate slightly from the rest of the population. Also, no such compositions were found in later studies.

The microtektite data set includes the major and trace element bulk compositions of 233 individual microtektites in the 100–800 μm size range (Glass et al., 2004; Glass and Koeberl, 2006; Folco et al., 2008, 2009, 2016, 2018; van Ginneken et al., 2018; Brase et al., 2021; Soens et al., 2021), with up to 678 μg/g Ni (Folco et al., 2018). They were recovered from 22 deep-sea sediment cores from the Indian, Pacific and Antarctic Oceans, and from 8 sediment traps in the Transantarctic Mountains and Sør Rondane Mountains, Antarctica. Microtektites are classified into chemical groups according to the classification first proposed by Glass et al. (2004): the most abundant normal-type with MgO < 6 wt% (n = 157), the less abundant high-Mg-type with MgO > 10 wt% (n = 15), intermediate-type with ~6–10 wt% (n = 21), and high-Ni-type with Ni > 100 μg/g and MgO < 6 wt% (n = 33), the rare high-Al-type with ~30–33 wt% Al_2O_3 and ~41–50 wt% SiO_2 (n = 5), and the unique high-Ni-Fe-type (SiO_2 = 55 wt%, FeO = 11 wt%, Ni = 214 μg/g). Major and trace element concentrations were determined by combining EPMA with INAA (Glass et al., 2004; Glass and Koeberl, 2006) or laser ablation – inductively coupled plasma – mass spectrometry, LA-ICP-MS (Folco et al., 2008, 2009, 2016, 2018; van Ginneken et al., 2018; Brase et al., 2021; Soens et al., 2021).

The data set also includes the analysis (by EPMA plus INAA) of the only shocked, partially melted, microscopic ejecta fragment found within the Australasian microtektite layer in core ODP 1144 for which a bulk composition is so far available (Glass and Koeberl, 2006). The fragment, approximately 1 mm in size, consists of mineral grains in a vesiculated glass matrix. It is dominated by fractured quartz up to 250 μm in maximum dimension, with lesser K-feldspar and plagioclase, and accessory zircon, rutile and ilmenorutile. Its major and trace element

bulk composition is similar to the (normal type) Australasian microtektites tektites. The fragment should represent a component of the still unknow target precursor material.

3. Results

Excluding the ten high-Mg type (as defined by Chapman and Scheiber, 1969), tektites have Mg concentrations ranging from 0.7 to 2.4 wt%, and Ni concentrations spanning two orders of magnitude from 4 to 428 μg/g (Fig. 2**A**). Nickel and Mg show a slight positive correlation defining a relatively high Ni/Mg trend, denominated T1. The trend roughly departs from the low-Ni-low-Mg composition of the UCC and ejecta fragment, with 51 tektites with Ni contents that are one order of magnitude higher (Ni > 100 μg/g) than crustal values (Ni ~ 20 μg/g). High-Mg tektites introduce some scatter at high Ni concentrations (Ni ~ 200 μg/g) with five tektites out of a total of ten with lower Ni/Mg ratios.

Microtektite compositions are distributed along two trends, where Ni and Mg are positively correlated departing from about UCC and ejecta fragment values: a high Ni/Mg trend and a low Ni/Mg trend (Fig. 2A). The first trend is the most populated one and defined by the majority of normal and the high-Ni microtektites (~80% of total number). It extends the high Ni/Mg trend T1 defined by tektites up to values of 680 μg/g Ni and 3.4 wt% Mg. The second low Ni/Mg trend, denominated T2**,** is defined by the microtektites with high contents of Mg. These are the less common microtektites belonging to the high-Mg- and the intermediate-types, with concentrations up to 33 μg/g Ni and ~13 wt% Mg. The rare (n = 4) high-Al microtektites in the data set also align along this low Ni/Mg T2 trend. Few normal type microtektites (n = 6; Ni < 70 μg/g), one high-Ni microtektite (Ni = 151 μg/g) and the only Fe-Ni-rich microtektite (Ni = 214 μg/g) in the data set form a weak and discontinuous array with Ni/Mg ratios intermediate between T1 and T2 in the Ni vs Mg space (Fig. 2A).

Terrestrial mafic and ultramafic rocks from various location worldwide (Frey and Prinz, 1978; Condie, 1993; Pearson et al., 2003) and volcanic rocks from Indochina (including the Bolaven volcanic plateau; Hung, 2010; Hoang et al., 2016; An et al., 2018; Sieh et al., 2020), containing up to ~2600 and ~350 μg/g Ni and ~28 and ~6 wt% Mg, show a positive relationship between Ni and Mg and define a trend with intermediate Ni/Mg ratio starting from UCC values (Fig. 2B). This trend is distinct from the main high Ni/Mg trend, T1, defined by tektites and the majority of normal- and high-Ni microtektites; it is also distinct from the secondary low Ni/Mg trend, T2, defined by high-Mg microtektites.

Remarkably, the high Ni/Mg trend, T1, observed in tektites, high-Ni microtektites and the bulk of normal microtektites lays along a mixing trend between UCC and chondritic values (full range: ~10,000–17,000 μg/g Ni and ~10–15 wt% Mg; Lodders and Fegley, 1998) in the Ni versus Mg space (compare Fig. 2A and 2B). A regression line set to intercept UCC values for the 85 specimens (both tektites and microtektites, except the 10 high-Mg tektites) in the T1 trend with Ni > 100 μg/g aligns with the UCC-chondrite mixing trend, despite some scatter ($R^2 = 0.35$; Fig. 2B).

4. Discussion

4.1. The chondritic origin of the Ni-rich component in tektites and microtektites

The observation that tektites (with the exception of 5 high-Mg ones) and the high-Ni and most of the normal microtektites – namely the bulk of the studied specimens – plot along a mixing trend between continental crust values and chondritic materials in the Ni versus Mg space (trend T1: Fig. 2A and B) provides evidence that the Ni-component in this set of specimens is a signature of a chondritic impactor and not a contribution of terrestrial mafic or ultramafic target rocks (e.g., Sieh et al., 2020). This observation also suggests that both UCC and ejecta fragment compositions are reasonable approximations of the bulk of the target precursor material end member, at least for the Mg and Ni contents considered here.

This result is consistent with previous detection of a broadly chondritic signature in the Cr/Ir ratios and unfractionated HSE distribution of 10 Ni-rich tektites (>150 μg/g Ni) selected from a batch of 92 Muong Nong and splash form specimens by Goderis et al. (2017), as well as with an extraterrestrial Os isotope signature independently detected in four high-Ni tektites (98–166 μg/g Ni) by Ackerman et al. (2019). It is also consistent with our previous work in which we identified a chondritic signature, possibly of LL ordinary chondrite composition (Fig. 2B), based on Ni, Co and Cr ratios in 33 high-Ni microtektites.

Mixing calculations (Fig. 2B) indicate a chondritic impactor contamination up to ~6% by weight for microtektites, with Ni contents up to ~680 μg/g (see also Table 4 and Fig. 6 in Folco et al., 2018), and up to ~4%, for tektites with Ni contents up to ~430 μg/g. Note that the concentrations of Ni in high-Ni microtektites would require up to ~30% mixing with a mafic terrestrial component. Such mixing would produce inconsistently high Mg contents, namely up to 7.5 Mg wt%. This value is 2.8 times higher than the average value for high-Ni Australasian tektites and microtektites of 2.7 Mg wt%, as already pointed out by Goderis et al. (2017), Folco et al. (2018) and Mizera (2022). Note also that Goderis et al. (2017) reported on non-chondritic Ni, Cr, Co ratios Cr/Ni 0.74, Co/Ni 0.08 and Cr/Co 8.42 (obtained through linear regression method), despite the chondritic Cr/Ir ratio and HSE distribution in the Australasian tektites they studied. They explained this geochemical signature as the reflection of either a chondritic impactor contribution that partly fractionated during impact, or a contamination of an impactor of primitive achondrite composition. Primitive achondrites are meteorites characterized by achondritic textures but quasi chondritic mineral and geochemical composition and, therefore, they have nearly unfractionated HSE patterns, similar to chondrites, but HSE abundances and Ni/Cr ratios which are distinctly higher than those of Earth's mantle. According to our new database, we observe that the Ni, Co and Cr interrelations are consistent with an impactor signature of broadly chondritic composition (Fig. 3). This is true not just for high-Ni microtektites, as discussed in detail in our previous work (Folco et al., 2018), but also for tektites, particularly those with high Ni contents in excess of 100 μg/g. The slope values of the regression lines for high-Ni tektites in the Cr/Ni, Co/Ni and Cr/Co spaces are 0.49, 0.06 and 7.8 respectively; those for high-Ni microtektites are 0.33, 0.05 and 8.04, respectively, despite a great deal of scatter. Those for chondritic materials (chondrites and primitive achondrites) range 0.12–0.38, 0.05–0.06 and 1.2–7.7, respectively (see Table 4 in Goderis et al., 2017, or Table 2 in Folco et al., 2018). The relatively small amount of projectile contamination explains, at least in part, the lack of a match of the Ni, Cr, Co ratios between tektites and chondritic materials reported by Goderis et al. (2017). Note that we arbitrarily assume UCC as endmember composition of the mixing because we do not know the actual composition of the target. By choosing the ejecta fragment as an alternative endmember, we would obtain a better fit of tektite and microtektite populations with chondritic materials in the Ni versus Co versus Cr space.

There is ample consensus that tektites and microtektites form through ultra-high temperature (and pressure) melting of the uppermost surface layers of Earth's crust (e.g., Stöffler et al., 2002; Ma et al., 2004; Rochette et al., 2018). This material is subject to chemical alteration due to weathering which, under specific environmental conditions, can produce passive enrichments of less mobile elements like Ni and parallel removal of mobile elements like Mg, particularly in soils containing a mafic or ultramafic rock component (e.g., Colin et al., 1990). A contribution of weathered mafic and ultramafic terrestrial rocks could possibly explain the high Ni/Mg T1 trend observed in tektites and the majority of microtektites. However, the lack of correlation between Ni and Al (Fig. 4) – the latter being a much less mobile element that typically accumulates in altered mafic and ultramafic lateritic soils (e.g., Colin et al., 1990) – makes this option unplausible.

Nickel has been found concentrated in rare microscopic Fe-Ni or Fe-

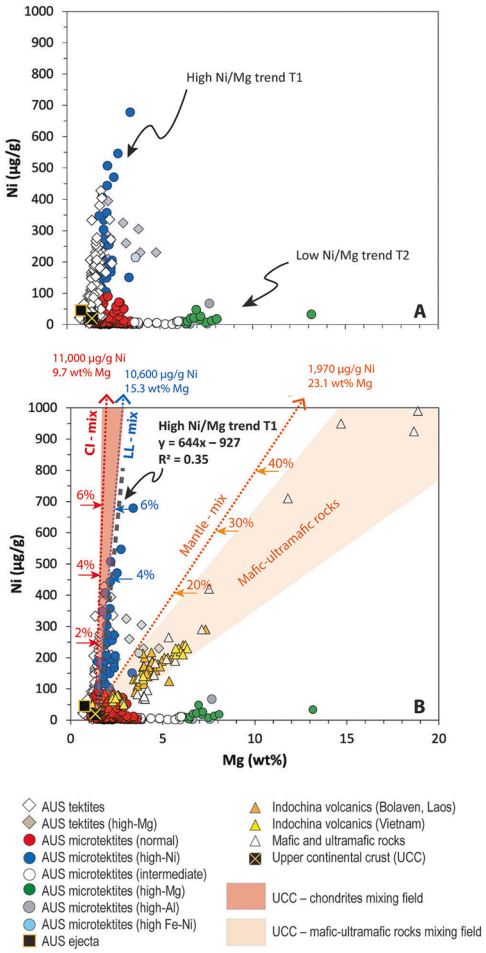

Fig. 2. Nickel (µg/g) versus Mg (wt%) variation diagrams for the 208 Australasian (AUS) tektites (227 individual analyses) and 230 microtektites (232 individual analyses) studied in this work (see Chapter 2 for references). Concentrations for the ejecta fragment in the microtektite layer from the ODP1444 core (Glass and Koeberl, 2006), the average UCC (Taylor and McLennan, 1995), the terrestrial mafic and ultramafic rocks (Condie, 1993; Frey and Prinz, 1978; Pearson et al., 2003) including the volcanic rocks from Indochina (An et al., 2018; Hoang et al., 2016; Hung, 2010; Sieh et al., 2020), are shown for comparison. A) Showing the two Ni/Mg trends observed in tektites and microtektites: the high Ni/Mg trend, T1 and the low Ni/Mg trend, T2. B) Showing the mixing trends between chondritic materials (here exemplified by the CI-chondrites with bulk Ni = 11000 µg/g and Mg = 9.70 wt%, and LL-chondrites with bulk Ni = 10600 µg/g and Mg = 15.3 wt%; e.g., Lodders and Fegley, 1998), Earth's mantle (Ni = 1960 µg/g and Mg = 22.8 wt%; Salters and Stracke, 2004) and terrestrial mafic and ultramafic rocks with the upper continental crust compositions. A regression line set to intercept UCC values for the 85 tektites and microtektites in the T1 trend with Ni > 100 µg/g is also shown (black dashed line). Note that there is a great deal of overlap between tektites and microtektites at low Ni and Mg values; tektites are thus plotted over microtektites in A, and vice-versa in B, to better show their distribution in the Ni versus Mg space.

Ni-S metallic spherules embedded in a few Australasian tektites (Chao et al., 1964; Křížová et al., 2019; Pan et al., 2023) and one may wonder if they contributed, at least in part, to the high-Ni component observed in Australasian tektites and microtektites. The Fe-Ni metallic spherules were reported in some Australasian tektite specimens from the Philippines, near Manila (Ortigas), and Vietnam, near Dalat (Chao et al., 1964). They are spheroids up to 800 µm in diameter consisting of Fe-Ni metal, occasionally including blebs of schreibersite and troilite. Nickel concentrations (EPMA) ranges from 4.7 to12.9 wt% in metal and from 12.1 to 15.8 wt% in schreibersite. Chao et al. (1964) proposed that the spherules were of meteoritic origin based on their close similarity with the meteoritic spheroids from Meteor Crater, Arizona, in terms of texture, mineral composition and nickel content. This interpretation was later questioned by Ganapathy and Larimer (1983) who observed patterns in the siderophile and highly siderophile element concentrations (INAA data) more closely related to terrestrial rocks than iron meteorites in two other metallic spherules. The Fe-Ni-S metallic spherules have been reported in Australasian tektites from Laos by Křížová et al. (2019) in four (out of the 31) Muon-Nong type specimens studied. Spherules are less than 10 µm in diameter and consist of the Ni-Fe sulfide shenzhuangite (chemical composition close to $NiFeS_2$, with Ni ~39 wt% and Co < 2 wt%; EPMA data). Whether the Ni-bearing sulfide inclusions represent a target or a meteoritic component trapped in tektite glass is still uncertain and requires further study, according to Křížová et al. (2019). Fe-Ni-S metallic spherules were also recently found in eight tektite specimens from Guangdong, Guangxi and Hainan Provinces, South China by Pan et al. (2023). Spherules are typically ~10 µm in diameter and mainly composed of Fe and S, and minor amounts of Ti, Ni, Co, Cr, and Mg, with Ni up to 4.4 wt% (EPMA data from five spherules). Because of their average Co/Ni ratio of ~0.11, which is similar with that of terrestrial materials (0.1–0.2; Ganapathy and Larimer, 1983) and distinct from that (<0.05) of typical Fe-S minerals in meteorites (e.g., Allen and Mason, 1973; Olsen et al., 1999), Pan et al. (2023) concluded that the Fe-S spherules most likely originated from iron-sulfides present in the target and not derived from the impactor. All the metallic spherules are nearly perfect spheres with quench textures indicating crystallization from immiscible metallic droplets in the silicate melt of the host tektite. They are not relic grains that survived impact melting. Geochemical fractionation between the metallic droplets and the host silicate-melt likely occurred as frequently observed in impact melts (e.g.,

Hamann et al., 2018; Folco et al., 2022). Regardless of the terrestrial versus meteoritic origin of their precursor materials, assessing whether or not they contributed, at least in part, to the high-Ni component observed in Australasian tektites and microtektites is impossible due to the lack information on the bulk composition of the host tektite specimens in terms of both Ni and Mg concentrations. It is however interesting to note that, despite the limited statistics and a great deal of scatter, the Fe-Ni and Fe-Ni-S spherules studied by Ganapathy and Larimer (1983) and Pan et al. (2023) define a positive correlation line with a slope value of 0.04 in the Co versus Ni space (Fig. SM1). This slope value is very close to the value of the Co/Ni ratio in chondritic or terrestrial mantle materials (~0.05–0.06) and distinct from terrestrial crust values which are one order of magnitude higher.

4.2. The origin of the Mg-rich component in microtektites

The low Ni/Mg T2 trend (Fig. 2) is populated only by a minority (~20%) of the studied microtektites, namely the high-Mg, the intermediate, the high-Al and few normal microtektites. The majority (73%; n = 30 out of 41) of the high-Mg, the intermediate and the high-Al microtektites are from Antarctica. The origin of this secondary trend could be studied in the context of disequilibrium melting and/or volatile fractionation during impact melting.

The low Ni/Mg T2 trend could represent variable degree of dilution of a Mg-rich end-member within the normal microtektite melt. In this view, Mg-rich microtektites likely formed from the physical separation of microscopic melt batches that could not completely homogenize with the normal microtektite melt prior to rapid melt fragmentation and quenching, in a context of disequilibrium mineral melting of a precursor which was compositionally heterogeneous at the submillimeter-scale.

In the attempt to constrain the Mg-rich end-member composition, we could consider the Mg-rich mineral phases in the target or in the impactor precursors with Mg contents in the 6 to 13 wt% range or higher. Unfortunately, we do not know where the crater is and, therefore, we do not know what the mineral and chemical composition of the target material exactly is. This is a significant limitation in the present discussion, nevertheless, we can assume that the relic mineral inclusions observed in tektites (Glass and Barlow, 1979) and microtektites (Folco et al., 2010a) and the mineral phases constituting the ejecta in the microtektite layer (Glass and Koeberl, 2006; Glass and Fries, 2008) likely represent components of the target material - possibly a fine-grained sedimentary deposit according to Glass and Barlow (1979). They are potential candidates of the tektite/microtektite target precursor material. Among them, Mg-bearing phases include garnet (Mg ~ 12 wt% in pyrope) and possibly pyroxene (Mg ~ 9–21 wt%), amphibole (Mg ~ 8 wt% in Mg-hornblende), chromite (Mg ~ 10 wt% in Mg-chromite), dolomite (Mg = 12.7 wt%) and micas Mg ~ 3.5–13.7 wt %). Assuming a chondritic impactor, potential impactor candidates include olivine (Mg up to 34 wt% in forsterite), pyroxene and Mg-chromite. Variation diagrams for a range of elements plotted against Mg are given in Fig. 5. Magnesium shows a broad positive correlation with Cr and Ni (although with a greater deal of scatter), and a negative correlation with Si. This suggests a Mg-olivine contribution to the mix (or its aqueous alteration products like serpentine minerals), likely from the chondritic precursor. The lack of a clear correlation between Mg and Al rules out micas, pyrope, and Mg-chromite. The lack of a correlation of Mg with Y and the negative correlation with Li confirm exclusion of pyrope and micas from the mix. Finally, the lack of correlation of Mg with Ca, Sc and Fe rules out a significant contribution of pyroxene and amphibole. Assuming mixing between UCC (Mg = 1.3 wt%) and an average chondritic olivine with Fo_{90} composition (Mg ~ 30 wt%), the olivine contribution to the average Mg content of ~7 wt% observed in high-Mg microtektites is ~20%. This addition implies a contribution of ~1 wt% Fe to the UCC compositional value of 3.5 wt% Fe (Taylor and McLennan, 1995) and is consistent with the average (3.3 ± 1.0 wt%) and maximum (6.0 wt%) Fe contents observed in high-Mg microtektites. Although geochemical data alone cannot rule out a terrestrial origin for the Mg-olivine endmember, the fact that no Mg-olivine has ever been found in tektites and microtektites and shocked ejecta in the microtektite layer (Glass and Barlow, 1979; Glass and Koeberl, 2006; Glass and Fries, 2008; Folco et al., 2010a) favors the interpretation of a meteoritic origin.

Evaporation/condensation play an important role in the chemical fractionation of Australasian microtektites during their formation process (e.g., Folco et al., 2010b; Howard, 2011). In particular, there is a trend of increasing depletion of volatiles with distance from the Indochina region, the putative impact location. This trend has been attributed to an increasing temperature–time regimes with increasing launch distance and thus impact energy (Folco et al., 2010b). Volatile alkali metals are generally depleted in high-Mg, intermediate and high-Al microtektites (e.g., Glass et al., 2004; Folco et al., 2010b; van Ginneken et al., 2018) and one may wonder if volatilization played a role in Mg fractionation. The common elements (i.e., neither refractory, nor volatiles) with condensation temperatures *Tc* comprised between 1290 and 1360 K (Lodders, 2003) like Co, Ni, Fe, Si, Cr and Mg do not covary despite their similar geochemical behavior during volatilization (Fig. 5): Co, Ni and Cr are positively correlated with Mg, whereas Si and Fe show negative or no correlation. In addition, although there is an overall negative correlation between Mg and volatile Li, Cs, Rb and K, no clear correlation between Mg and volatile Na is observed. Likewise, while there is a positive correlation between Mg and refractory Cr, there is no clear correlation between Mg and refractory Y, Sc, Al, Ti and Zr. We therefore conclude that volatilization did not play a significant role in the formation of the low Ni/Mg T2 trend in Australasian microtektites. Future investigations should focus on a larger number of microtektites with Mg contents above 8 wt% to check the correlations discussed above.

4.3. A possible terrestrial mafic component in high-Mg tektites and microtektites with intermediate Ni/Mg ratio

The discontinuous alignment of very few normal microtektites, one high-Ni microtektite and the only high-Fe-Ni microtektite in the collection described above could identify an additional yet secondary trend with intermediate Ni/Mg ratio. In a context of incomplete melt homogenization prior to melt fragmentation described above, this secondary trend could be evidence of minor terrestrial contribution to the Ni-component in the microtektites since it lays on the mixing trend between continental crustal material and mafic and ultramafic terrestrial rocks in the Ni vs Mg space (Fig. 2). The five (out of the ten) high-Mg tektites (Chapman and Scheiber, 1969) with high Ni contents around 200 – 300 μg/g, plotting between the high Ni/Mg T1 chondritic trend and the terrestrial of mafic and ultramafic rocks with intermediate Ni/Mg, may also record some terrestrial contribution to the Ni-component. The fact the Ni-rich component in Australasian tektites and microtektites is not merely sourced by the chondritic impactor, but also, although to a lesser extent, by terrestrial mafic or ultramafic target rocks, requires heterogeneous admixture of felsic and mafic components in the target material, variable degrees of projectile-target interaction and consequent formation of geochemically diverse batches of impact melt.

4.4. Constraining the impactor type

The Ni versus Mg relationship in Australasian tektites and microtektites presented in this work shows that the high-Ni component – at least in the great majority of them – is a signature of a chondritic impactor, consistently with previous works on tektites (Goderis et al., 2017; Ackerman et al., 2019) and microtektites (Folco et al., 2018). These three works document that the chondritic impactor is detectable in those specimens enriched in Ni with concentrations up to few hundreds of μg/g or more. Of the thousands of Australasian tektites present

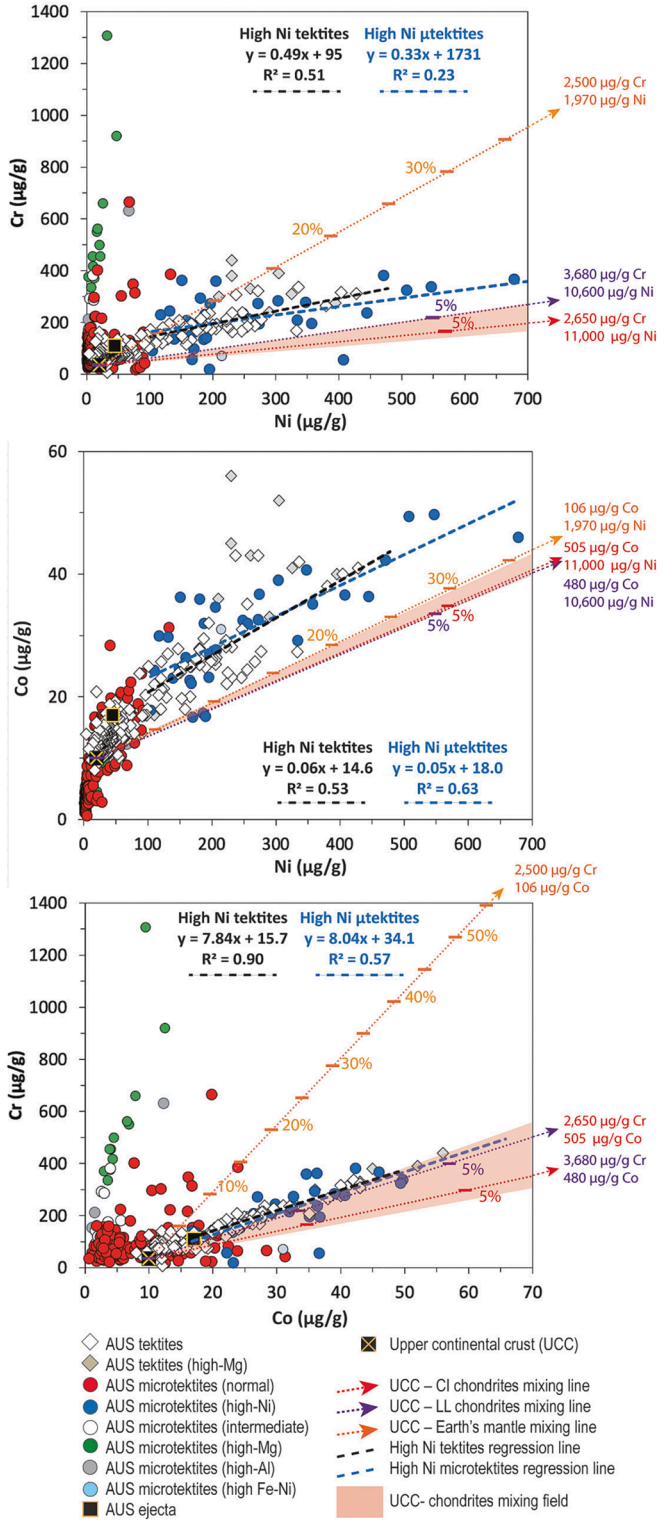

Fig. 3. Cr-Co-Ni relations in Australasian (AUS) tektites and microtektites. Concentrations for the average UCC (Taylor and McLennan, 1995) and the ejecta fragment in the microtektite layer from the ODP1444 core (Glass and Koeberl, 2006) are shown for comparison. Dotted lines are mixing lines between UCC and CI (red) and LL (purple) chondrites (Lodders and Fegley, 1998), and Earth's mantle (ginger; Salters and Stracke, 2004). Dashed lines are regression lines for high-Ni tektites (black) and microtektites (blue) with Ni contents in excess of 100 µg/g.

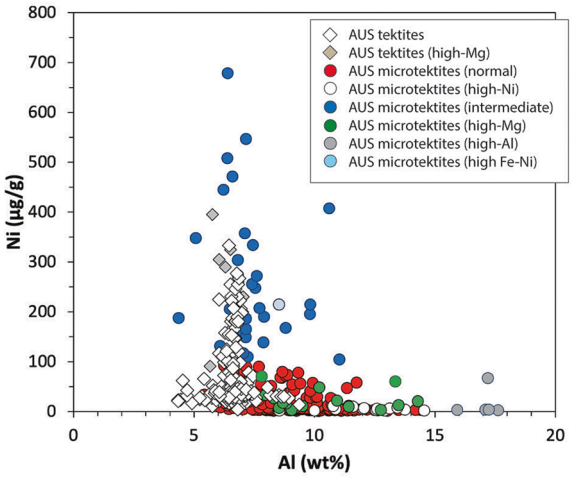

Fig. 4. Nickel versus Al variation diagram for Australasian (AUS) tektites and microtektites. Note the lack of correlation between Ni and Al.

in various research collections worldwide, specimens with this geochemical signature are rather rare, but their potential in constraining the impactor type is worth continuing extensive geochemical surveys.

In our previous work on Ni, Cr and Co ratios in Australasian microtektites (Folco et al., 2018), we performed mixing calculations between crustal and chondritic compositions in the attempt to constrain the chondritic impactor type. Despite substantial overlap in Cr/Ni versus Co/Ni values for several meteorite types with primitive compositions (ordinary, carbonaceous and enstatite chondrites, and primitive achondrites), calculations suggest an ordinary chondrite, possibly belonging to the LL class as the best fit; however, an L chondrite or a CK chondrite are plausible alternatives (withing the uncertainty of the method). This latter uncertainty could be significantly reduced by studying Cr-isotope systematics in high-Ni tektites. Cr-isotopes are in fact expected to discriminate between ordinary and carbonaceous chondrite signatures (e.g., Koeberl et al., 2007).

The importance of the combined use of different geochemical and isotopic methods for constraining the impactor type in impact melt rocks bearing a meteoritic signature, mainly siderophile Ni, Co and Cr, HSE, Os-, O- and Cr-isotope systematics, has been largely discussed in previous work (e.g., Koeberl et al., 2012; Goderis et al., 2013; Magna et al., 2017; Folco et al, 2018). Successful examples combining Cr-isotopes and siderophile interelement ratios are, for instance, the studies of the impact melt-rocks from the Lappajärvi (Finland) and Clearwater East (Canada) impact craters (Koeberl et al., 2007), from the Zamanshin impact structure (Kazakhstan; Jonášová et al., 2016; Magna et al., 2017) or the Central American belizites (Rochette et al., 2021). A further example is given by some Ivory Coast tektites enriched in siderophile elements (Koeberl and Shirey, 1993). Here a meteoritic component (<1% by weight) was first detected based on Os isotope analysis, although discrimination between a chondritic or iron meteorite signature could not be possible due to intrinsic limitations of the method. Nevertheless, guided by these results, an ordinary chondritic signature was later constrained through Cr-isotope analysis of the very same tektite specimens (Koeberl et al., 2007). Checking Cr-isotope composition in high-Ni Australasian tektites as proposed above would be instrumental to test the use of Mg, Ni, Cr and Co interrelations in confirming the identification of an impactor component, as performed in the present work, and in constraining the impactor type. Unfortunately, testing the use of Mg, Ni, Cr and Co interrelations in Ivory Coast tektites and microtektites is problematic due to the limited database available so far (e.g., Jones, 1985; Koeberl et al., 1997; Glass et al., 2004).

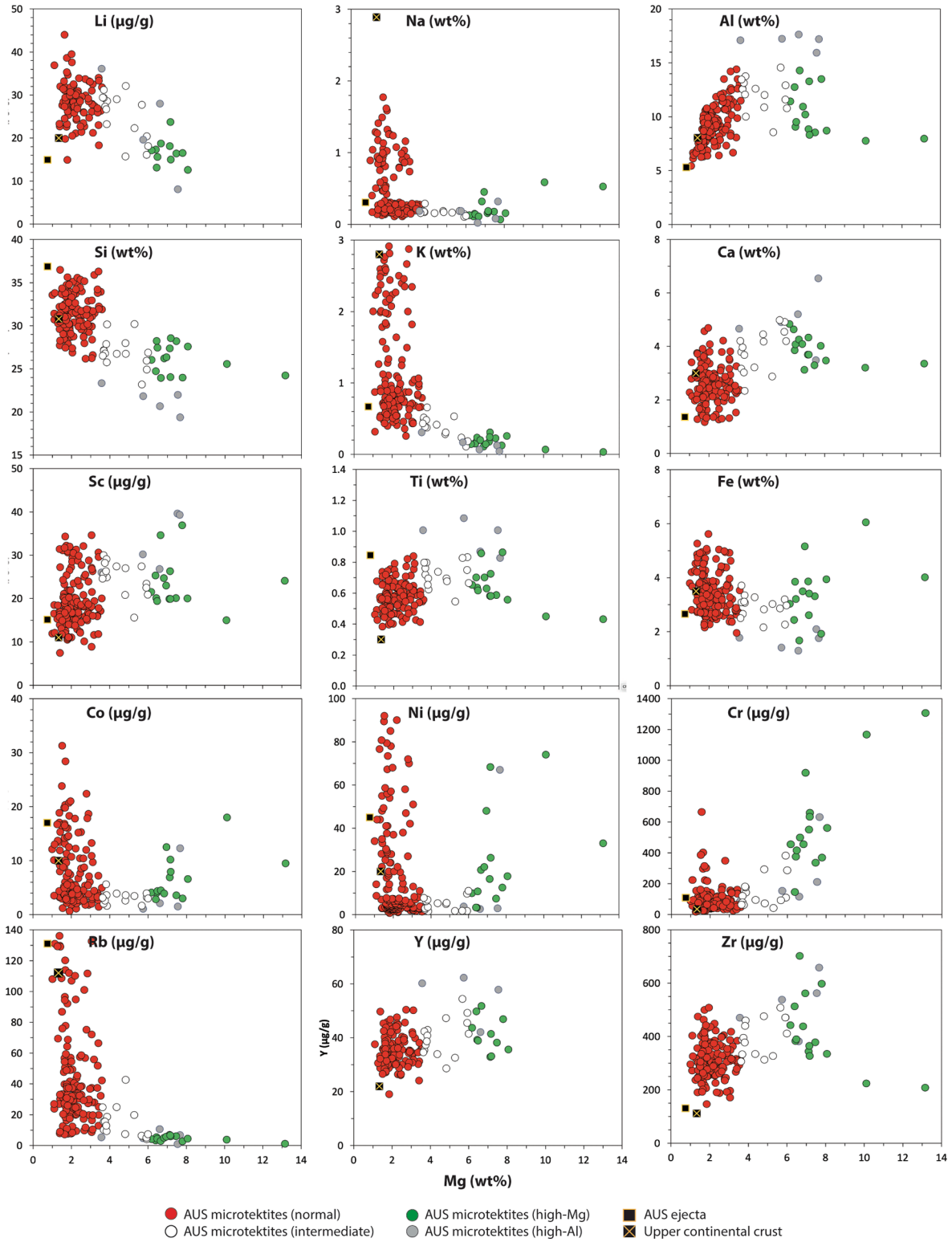

Fig. 5. Variation diagrams for a range of elements plotted against Mg for Australasian microtektites defining the low Ni/Mg trend, T2, and belonging to the high-Mg, intermediate and high-Al types. Data for normal type Australasian microtektites (this work), an ejecta fragment in the microtektite layer from the ODP1444 core, and the average UCC composition are plotted for comparison. Elements are arranged according to increasing mass.

5. Conclusions

We have studied the Ni-Mg interrelations in Australasian tektites and microtektites using a large database from the literature (208 tektites and 238 microtektites). The Ni-Mg interrelations show that the Ni-rich component in high-Ni tektites and microtektites with high Ni/Mg ratio is the signature of an impactor of chondritic composition in a parent impact melt of broadly UCC composition, and not a mafic terrestrial component in the target. This strengthens previous works on high-Ni tektites (Goderis et al., 2017; Ackerman et al., 2019) and microtektites (Folco et al., 2018). A chondritic component up to 4% and 6% by weight is estimated in tektites and microtektites, respectively, based on Ni-Mg

mixing calculations. A terrestrial mafic component maybe identified in some specimens like some high-Mg tektites (as defined by Chapman and Scheiber, 1969) and in a minority of microtektites with intermediate Ni/Mg ratios. These compositional differences are likely the combined result of target heterogeneity and variable degrees of impactor-target melt interaction involving mixing of three main components: dominant felsic rocks in the target, lesser mafic rocks in the target, and the chondritic impactor.

There is a greater compositional variability in microtektites relative to tektites in the Ni versus Mg space. This is likely the result of incomplete homogenization of heterogeneous impactor and target precursor materials at the microtektite scale in the context of disequilibrium impact melting and rapid melt fragmentation during ejection. This disequilibrium process can explain the high-Mg (and low-Ni/Mg) compositional type within the microtektite population.

High-Ni (Ni $>$ 100 μg/g) tektites and microtektites present in research collections worldwide are thus expected to reveal the chondritic impactor type that generated the Australasian strewn field through the combination of geochemical and isotopic analysis. This will provide significant input for reconstructing the scenario of one of the most catastrophic and elusive impacts in the Cenozoic. It could also contribute to a better understanding of several still unclear aspects of tektite formation process, such as the target-impactor physical interaction and elemental fractionation.

Declaration of Competing Interest

The authors declare that they have no known competing financial interests or personal relationships that could have appeared to influence the work reported in this paper.

Acknowledgements

Tektite and microtektite research at Pisa University is funded through grants MIUR: PNRA16_00029 Meteoriti Antartiche. We appreciate constructive reviews by Aaron Cavosie, Jiří Mizera, Christopher Hamann and Steven Goderis. We also thank Associate Editor Tomas Magna for handling the manuscript.

Appendix A. Supplementary material

Including two tables reporting major and trace element compositions (element wt% and μg/g, respectively) of Australasian tektites (Table SM1) and microtektites (Table SM2) from the literature studied in this work (see main text for references), and one figure (Figure SM1) showing a Co versus Ni plot for Fe-Ni and Fe-S-Ni spherule inclusions in Australasian tektites (see figure caption for references). Supplementary material to this article can be found online at https://doi.org/10.1016/j.gca.2023.09.018.

References

Ackerman, L., Skála, R., Křížová, Š., Žák, K., Magna, T., 2019. The quest for an extraterrestrial component in Muong Nong-type and splash-form Australasian tektites from Laos using highly siderophile elements and Re-Os isotope systematics. Geochim. Cosmochim. Acta 252, 179–189.

Allen, R.O.J., Mason, B., 1973. Minor and trace elements in some meteoritic minerals. Geochim. Cosmochim. Acta 37, 1435–1456.

Amare, K., Koeberl, C., 2006. Variation of chemical composition in Australasian tektites from different localities in Vietnam. Meteorit. Planet. Sci. 41, 107–123.

An, A.-R., Choi, S.H., Yu, Y., Lee, D.-C., 2018. Petrogenesis of Late Cenozoic basaltic rocks from southern Vietnam. Lithos 272–273, 192–204.

Brase, L.E., Harvey, R.P., Folco, L., Suttle, M.D., McIntosh, E.C., Day, J.M.D., Corrigan, C. M., 2021. Microtektites and glassy spherules from new sites in the Transantarctic Mountains. Antarctica. Meteorit. Planet. Sci. 56, 829–843.

Cavosie, A.J., Timms, N.E., Erickson, T.M., Koeberl, C., 2017. New clues from Earth's most elusive impact crater: Evidence of reidite in Australasian tektites from Thailand. Geology 46 (3), 203–206.

Chao, E.C.T., Dwornik, E.J., Littler, J., 1964. New data on the nichel-iron spherules from Southeast Asian tektites and their implications. Geochim. Cosmochim. Acta 28, 971–980.

Chapman, D.R., Scheiber, L.C., 1969. Chemical investigation of Australasian tektites. J. Geophys. Res. 74, 6737–6776.

Colin, F., Nahon, D., Trescases, J.J., Melfi, J., 1990. Lateritic weathering of Pyroxenites at Niquelandia, Goias, Brazil: The supergene behavior of Nickel. Chem. Geol. 85, 1010–1023.

Condie, K.C., 1993. Chemical Composition and Evolution of the Upper Continental Crust; Contrasting Results from Surface Samples and Shales. Chem. Geol. 104, 1–37.

Di Vincenzo, G., Folco, L., Suttle, M., Brase, L., Harvey, R., 2021. Multi-collector 40Ar-39Ar dating of microtektites from Transantarctic Mountains (Antarctica): a definitive link with the Australasian tektite/microtektite strewn field. Geochim. Cosmochim. Acta 298, 112–130.

Ebert, M., Hecht, L., Deutsch, A., Kenkmann, T., Wirth, R., Berndt, J., 2014. Geochemical processes between steel projectiles and silica-rich targets in hypervelocity impact experiments. Geochim. Cosmochim. Acta 133, 257–279.

Fazio, A., D'Orazio, M., Cordier, C., Folco, L., 2016. Target-projectile interaction during impact melting at Kamil Crater, Egypt. Geochim. Cosmochim. Acta 18, 33–50.

Folco, L., Rochette, P., Perchiazzi, N., D'Orazio, M., Laurenzi, M., Tiepolo, M., 2008. Microtektites from Victoria Land Transantarctic Mountains. Geology 36, 291–294.

Folco, L., D'Orazio, M., Tiepolo, M., Tonarini, S., Ottolini, L., Perchiazzi, N., Rochette, P., Glass, B.P., 2009. Transantarctic Mountain microtektites. Geochemical affinity with Australasian microtektites. Geochim. Cosmochim. Acta 73, 3694–3722.

Folco, L., Perchiazzi, N., D'Orazio, M., Frezzotti, M.L., Glass, B., Rochette, P., 2010a. Shocked quartz and other mineral inclusions in Australasian microtektites. Geology 38, 211–214.

Folco, L., Glass, B.P., D'Orazio, M., Rochette, P., 2010b. A common volatilization trend in Transantarctic Mountain and Australasian microtektites: Implications for their formation model and parent crater location. Earth Planet. Sci. Lett. 293, 135–139.

Folco, L., Carone, L., D'Orazio, M., Cordier, C., Suttle, M.D., van Ginneken, M., Masotta, M., 2022. Microscopic impactor debris at Kamil Crater (Egypt): The origin of the Fe-Ni oxide spherules. Geochim. Cosmochim. Acta 335, 297–322.

Folco, L., D'Orazio, M., Gemelli, M., Rochette, P., 2016. Stretching out the Australasian microtektite strewn field in Victoria Land Transantarctic Mountains. Polar Sci. 10, 147–159.

Folco, L., Glass, B.P., D'Orazio, M., Rochette, P., 2018. Impactor identification in Australasian microtektites based on Cr, Co and Ni ratios. Geochim. Cosmochim. Acta 222, 550–568.

Frey, F.A., Prinz, M., 1978. Ultramafic Inclusions from S. Carlos, Arizona: Petrologic and geochemical data bearing on their petrogenesis. Earth Planet. Sci. Lett. 38, 129–176.

Gall, L., Williams, H.M., Halliday, A.N., Kerret, A.C., 2017. Nickel isotopic composition of the mantle. Geochim. Cosmochim. Acta 199, 196–209.

Ganapathy, R., Larimer, J.W., 1983. Nickel-iron spherules in tektites: non-meteoritic in origin. Earth Planet. Sci. Lett. 65, 225–228.

Gattacceca, J., Rochette, P., Quesnel, Y., Singsoupho, S., 2021. Revisiting the paleomagnetism of Muong Nong layered tektites: Implications for their formation process. Meteorit. Planet. Sci. 57, 558–571.

Glass, B.P., Barlow, R.A., 1979. Mineral inclusions in Muong Nong-type indochinites: implications concerning parent material and process of formation. Meteoritics 14, 55–67.

Glass, B.P., Fries, M., 2008. Micro-Raman spectroscopic study of fine-grained, shock-metamorphosed rock fragments from the Australasian microtektite layer. Meteorit. & Planet. Sci. 43, 1487–1496.

Glass, B.P., Simonson, B.M., 2013. Distal Impact Ejecta Layers. A Record of Large Impacts in Sedimentary Deposits. Springer, Heidelberg, New York, Dordrecht, London.

Glass, B.P., Huber, H., Koeberl, C., 2004. Geochemistry of Cenozoic microtektites and clinopyroxene-bearing spherules. Geochim. Cosmochim. Acta 68, 3971–4006.

Glass, B.P., Koeberl, C., 2006. Australasian microtektites and associated impact ejecta in the South China Sea and the Middle Pleistocene supereruption of Toba. Meteorit. Planet. Sci. 41, 305–326.

Glass, B.P., Pizzuto, J.E., 1994. Geographic variation in Australasian microtektite concentrations: implications concerning the location and size of the source crater. J. Geophys. Res. 99, 19075–19081.

Goderis, S., Paquay, F., Claeys, P., 2013. Projectile identification in terrestrial impact structures and ejecta material. In: Osinski, G.R., Pierazzo, E. (Eds.), Impact Cratering - Processes and Products. Wiley-Blackwell, Oxford, pp. 223–239.

Goderis, S., Tagle, R., Fritz, J.D., Bartoschewitz, R., Artemieva, N., 2017. On the nature of the Ni-rich component in splashform Australasian tektites. Geochim. Cosmochim. Acta 217, 28–50.

Hamann, C., Fazio, A., Ebert, M., Hecht, L., Folco, L., Deutsch, A., Wirth, R., Reimold, W. U., 2018. Silicate liquid immiscibility in impact melts. Meteorit. Planet. Sci. 53, 1594–1632.

Hoang, N., Huong, T.T., Bac, D.T., Vu, N.V., Thu, N.T., Thang, C.S., Dang, P.T., 2016. Magma source feature and eruption age of volcanic rocks in the Tram Tau district, Tu Le Basin, Vietnam. J. Earth Sci. 38, 242–255.

Howard, K.T., 2011. Volatile enhanced dispersal of high velocity impact melts and the origin of tektites. Proc. Geol. Ass. 122, 363–382.

Hung, K.T., 2010. Overview of the magmatism in northwestern Vietnam. Ann. Soc. Geol. Pol. 80, 185–226.

Jonášová, Š., Ackerman, L., Žák, K., Skála, R., Ďurišová, J., Deutsch, A., Magna, T., 2016. Geochemistry of impact glasses and target rocks from the Zhamanshin impact structure, Kazakhstan: Implications for mixing of target and impactor matter. Geochim. Cosmochim. Acta 190, 239–264.

Jones, W.B., 1985. Chemical analyses of Bosumtwi crater target rocks compared with the Ivory Coast tektites. Geochim. Cosmochim. Acta 49, 2569–2576.

Jourdan, F., Nomade, S., Wingate, M.T.D., Eroglu, E., Deino, A., 2019. Ultraprecise age and formation temperature of the Australasian tektites constrained by 40Ar/39Ar analyses. Meteorit. Planet. Sci. 54, 2573–2591.
Koeberl, C., Shirey, S.B., 1993. Detection of a meteoritic component in Ivory Coast tektites with rhenium–osmium isotopes. Science 261, 595–598.
Koeberl, C., Bottomley, R., Glass, B.P., Storzer, D., 1997. Geochemisry and age of Ivory Coast tektites and microtektites. Geochim. Cosmochim. Acta 61, 1745–1772.
Koeberl, C., Shukolyukov, A., Lugmair, G.W., 2007. Chromium isotopic studies of terrestrial impact craters: identification of meteoritic components at Bosumtwi, Clearwater East, Lappajärvi, and Rochechouart. Earth Planet. Sci. Lett. 256, 534–546.
Koeberl, C., Claeys, P.h., Hecht, L., McDonald, I., 2012. Geochemistry of impactites. Elements 8, 37–42.
Křízová, Š., Skála, R., Halodová, P., Žák, K., Ackerman, L., 2019. Near end-member shenzhuangite, $NiFeS_2$, found in Muong Nong-type tektites from Laos. Am. Mineral. 104, 1165–1172.
Lodders, K., 2003. Solar system abundances and condensation temperatures of the elements. Astrophys. J. 591, 1220–1247.
Lodders, K., Fegley, B., 1998. The Planetary Scientist's Companion. Oxford Univ. Press, New York.
Ma, P., Aggrey, K., Tonzola, C., Schnabel, C., De Nicola, P., Herzog, G.F., Wasson, J.T., Glass, B.P., Brown, L., Tera, F., Middleton, R., Klein, J., 2004. Beryllium-10 in Australasian tektites: constraints on the location of the source crater. Geochim. Cosmochim. Acta 68, 3883–3896.
Magna, T., Žák, K., Pack, A., Moynier, F., Mougel, B., Peters, F., Skála, R., Jonášová, Š., Mizera, J., Řanda, Z., 2017. Zhamanshin astrobleme provides evidence for carbonaceous chondrite and post-impact exchange between ejecta and Earth's atmosphere. Nat. Commun. 8, 227.
Masotta, M., Peres, S., Folco, L., Mancini, L., Rochette, P., Glass, B.P., Campanale, F., Gueninchault, N., Radica, F., Singsoupho, S., Navarro, E., 2020. 3D X-ray tomographic analysis reveals how coesite is preserved in Muong Nong-type tektites. Sci. Rep. 10, 20608.
Mizera, J., 2022. Quest for the Australasian impact crater: Failings of the candidate location at the Bolaven Plateau, Southern Laos. Meteorit. Planet. Sci. 57, 1973–1986.
Mizera, J., Řanda, Z., Strunga, V., Klokočník, J., Kostelecký, J., Bezděk, A., Moravec, Z., 2022. Parent crater for Australasian tektites beneath the sands of the Alashan Desert, Northwest China: Best candidate ever? In: Foulger, G. R., Hamilton, L. C., Jurdy, D. M., Stein, C. A., Howard, K. A., Stein, S., (Eds.), In the Footsteps of Warren B. Hamilton: New Ideas in Earth Science. Geol. Soc. Am. Spec. Pap. 553, 323–334.
Mizera, J., Řanda, Z., Kameník, J., 2016. On a possible parent crater for Australasian tektites: Geochemical, isotopic, geographical and other constraints. Earth Sci. Rev. 154, 123–137.
Olsen, E.J., Kracher, A., Davis, A.M., Steele, I.M., Hutcheon, D.I., Bunch, T.E., 1999. The phosphates of IIIAB iron meteorites. Meteorit. Planet. Sci. 34, 285–300.
Pan, Q., Xiao, Z., Wu, Y., Shi, T., Yin, Z., Yan, P., Li, Y., 2023. Magnetic properties of Australasian tektites from South China. J. Geophys. Res.: Solid Earth 128, e2022JB025269.
Pearson, G., Canil, D., Shirey, S.B., 2003. Mantle samples included in volcanic rocks: xenoliths and diamonds. In: Holland, H.D., Turekian, K.K. (Eds.), Treatise on Geochemistry, vol. 2, pp. 171–275.
Prasad, M.S., Mahale, V.P., Kodagali, V.N., 2007. New sites of Australasian microtektites in the central Indian Ocean: Implications for the location and size of source crater. J. Geophys. Res. 112, E06007.
Rochette, P., Braucher, R., Folco, L., Horng, C.S., Aumaître, G., Bourlès, D.L., Keddadouche, K., 2018. ^{10}Be in Australasian Microtektites Compared to Tektites: Size and Geographic Controls. Geology 46, 803–806.
Rochette, P., Beck, P., Bizzarro, M., Braucher, R., Cornec, J., Debaille, V., Devouard, B., Gattacceca, J., Jourdan, F., Moustard, F., Moynier, F., Nomade, S., Reynard, B., 2021. Impact glasses from Belize represent tektites from the Pleistocene Pantasma impact crater in Nicaragua. Commun. Earth Environ. 2, 94.
Salters, V.J.M., Stracke, A., 2004. Composition of the depleted mantle. Geochem. Geophys. Geosystems 5, Q05B07.
Schmitz, B., 2013. Extraterrestrial spinels and the astronomical perspective on Earth's geological record and evolution of life. Chem. Erde 73, 117–145.
Schwarz, W.H., Trieloff, M., Bollinger, K., Gantert, N., Fernandes, V.A., Meyer, H.P., Povenmire, H., Jessberger, E.K., Guglielmino, M., Koeberl, C., 2016. Coeval ages of Australasian, Central American and Western Canadian tektites reveal multiple impacts 790 ka ago. Geochim. Cosmochim. Acta 178, 307–319.
Shirai, N., Ackter, R., Ebihara, M. 2016. Precursor materials of Australasian tektites in light of chemical composition. 47th Lunar Planet. Sci. Conf., abstract No. 1847.
Sieh, K., Herrin, J., Jicha, B., Angel, D.S., Moore, J.D.P., Banerjee, P., Wiwegwin, W., Sihavong, V., Singer, B., Chualaowanich, T., Charusiri, P., 2020. Australasian impact crater buried under the Bolaven Volcanic field, Southern Laos. Proc. Natl. Acad. Sci. U.S.A. (12/2019), 1–8.
Soens, B., van Ginneken, M., Chernonozhkin, S., Slotte, N., Debaille, V., Vanhaecke, F., Terryn, H., Claeys, P., Goderis, S., 2021. Australasian microtektites across the Antarctic continent: Evidence from the Sør Rondane Mountain range (East Antarctica). Geosci. Front. 12, 101153.
Son, T.H., Koeberl, C., 2005. Chemical variation within fragments of Australasian tektites. Meteorit. Planet. Sci. 40, 805–815.
Stöffler, D., Artemieva, N.A., Pierazzo, E., 2002. Modeling the Ries-Steinheim impact event and the formation of the moldavite strewn field. Meteorit. Planet. Sci. 37, 1893–1907.
Tagle, R., Claeys, P., 2005. An ordinary chondrite as impactor for the Popigai crater, Siberia. Geochim. Cosmochim. Acta 69, 2877–2889.
Taylor, S.R., McLennan, S.M., 1995. The geochemical evolution of the continental crust. Rev. Geophys. 32, 241–265.
van Ginneken, M., Genge, M.J., Harvey, R.P., 2018. A new type of highly-vaporized microtektite from the Transantarctic Mountains. Geochim. Cosmochim. Acta 228, 81–94.
Wasson, J.T., 1991. Layered tektites: a multiple impact origin or the Australasian tektites. Earth Planet. Sci. Lett. 102, 95–109.
Žák, K., Skála, R., Pack, A., Ackerman, L., Křízová, Š., 2019. Triple oxygen isotope composition of Australasian tektites. Meteorit. Planet. Sci. 54, 1167–1181.